Estimating Bottom Stress on Continental Shelves from Tidal and Wave Models

Uehara, Katsuto
Research Institute for Applied Mechanics, Kyushu University

https://doi.org/10.15017/27139

出版情報：九州大学応用力学研究所所報. 143, pp.69-73, 2012-09. Research Institute for Applied Mechanics, Kyushu University

Estimating Bottom Stress on Continental Shelves from Tidal and Wave Models

Katsuto UEHARA[*1]
E-mail of corresponding author: *uehara@riam.kyushu-u.ac.jp*
(Received July 31, 2012)

Abstract

A numerical model was developed to estimate bottom stresses induced by waves and tides, in order to obtain multiyear statistics on the occurrence of sediment resuspension over the continental shelf. The model consists of a tidal module which predicts tidal currents at level 1m above the seabed by employing 20 tidal constituents, and a wave module supplying near-bottom orbital velocities averaged over a wave spectrum. Predicted waves and tides were combined to provide bottom stress estimations at the temporal interval of one hour. The model was tested at the Yellow/East China Sea and compared with observations. Tidal currents and wave heights predicted in the model was consistent with observations, and the temporal pattern of predicted bottom stress matched with that of suspended sediment concentrations observed. It was found that the temporal resolution of several hours is required to resolve extreme events which cause resuspensions and that tidal constituents other than M_2 would be necessary to reproduce tidal currents used in the bottom stress estimation.

Key words : Sediment resuspension, East China Sea, Yellow Sea, Numerical model

1. Introduction

The continental shelf is a shallow sea attached to lands which acts as an interface for the material exchange between lands and the ocean. Previous studies indicate that sediments discharged from rivers often experience depositions and resuspensions at the shelf region before being transported into outer oceans[1),2)]. Unlike deep ocean where deposition dominates resuspension, the impact of sediment resuspension on the continental shelf, causing upward material flux from the seabed toward the overlying seawater, should be taken into account when estimating the material budget over the shelf, as its seabed is prone to strong dynamical processes such as waves and tides.

Nevertheless, statistics on the shelf-wide occurrence of the sediment resuspension are not fully understood because the process is associated with extreme events which is not easy to be observed. Furthermore, previous numerical models dealing with shelf-wide sediment transports often use climatological winds which do not resolve extreme events to predict waves and currents[3)], or apply realistic wind forcing over a limited duration[4)]. In addition, the tidal module of many models deals only with the M_2 constituent[5)], which will be shown to be insufficient for the case of the Yellow/ East China Sea, the seventh largest continental shelf in the world.

This report describes a numerical procedure to estimate bottom stresses caused by waves and tides, which may be related to the occurrence of sediment resuspension on continental shelves. The scheme is designed to estimate the bottom-stress field over the shelf for the duration longer than a year in the temporal resolution of one hour. Here our focus is on introducing the model formulation and presenting its performance in comparison to observations. Application to actual problems will be described elsewhere.

2. Methods

We estimated bottom stresses under the presence of waves and tidal currents. As the estimation requires near-bottom tidal currents and near-bottom orbital velocities of waves, numerical models on tides and waves have been introduced as described below.

2.1 Tidal model

A two-dimensional finite-difference model was employed to predict depth-averaged tidal currents in the continental shelf seas. Governing equations are:

$$\partial\eta/\partial t + \nabla \cdot (D\mathbf{u}) = 0 \tag{1}$$

*1 Research Institute for Applied Mechanics, Kyushu University

$$\partial D\mathbf{u}/\partial t + (\mathbf{u}\cdot\nabla)D\mathbf{u} + \mathbf{k}(2\Omega\sin\varphi)\times D\mathbf{u} = -gD\nabla(\eta-\eta_e) - c_D|\mathbf{u}|\mathbf{u} + A_h D\nabla^2\mathbf{u} \quad (2)$$

where t is time, ∇ the horizontal gradient operator, η the surface elevation, $\mathbf{u}$ the depth-averaged current vector, $D = H + \eta$, H the undisturbed depth, Ω the angular velocity of the Earth's rotation, φ the latitude, $\mathbf{k}$ the vertical unit vector, g the acceleration due to gravity, η_e the tide-generating potential, c_D a quadratic bottom friction coefficient (=0.0020), A_h the horizontal eddy-viscosity coefficient (=100 m^2/s), respectively.

The equations were discretized on a staggered grid of Arakawa C-type with a resolution of 1/12 degrees. Tides were driven primarily by surface elevation along open boundaries derived from the harmonic constants of 16 constituents (M_2, S_2, K_1, O_1, N_2, P_1, K_2, Q_1, M_1, J_1, OO_1, $2N_2$, μ_2, ν_2, L_2 and T_2) of a global model (TPXO.7.2) and by tidal potential η_e in equation (2) compiled from the harmonic constants of 5 constituents (M_2, S_2, K_1, O_1 and N_2). The numerical scheme to manipulate open boundaries were based on Bills and Noye (1987)[6].

Model runs were made for 225.92 days, and the last 205.92 days of which were used to estimate harmonic constants of 20 constituents (16 forcing components plus four shallow-water components, i.e., M_4, SM_4, M_3 and M_6). When estimating the bottom stress, depth-averaged tidal currents at arbitrary time periods were retrieved by recombining these harmonic constants.

2.2 Near-bottom tidal currents

The depth-averaged tidal currents estimated by the tidal model were converted to tidal currents at level 1m above the seafloor as the bottom stress estimation require such quantities. The conversion process was based on Soulsby (1983)[7] which considers the difference in the thickness of bottom boundary layers associated with cyclonic and anti-cyclonic components of tidal currents. The no-slip bottom boundary condition was applied at the finite height $z = z_0 = 0.5$mm, instead of at $z = 0$ (bottom), to avoid singularity in the solution. It was also assumed that the depth-averaged current speed represents the tidal speed at $z_M = 0.32D$, where D is the water depth.

In the present formulation, we assume that the vertical eddy viscosity K increases linearly with height as $K = \kappa\hat{u}_* z$, where κ is the Karman constant (=0.40), $\hat{u}_* = \sqrt{c_D}|u_a|$ the maximum friction velocity in a tidal cycle, $|u_a|$the amplitude of the largest tidal harmonic constituents (usually the M_2 constituent). Then the anti-clockwise (denoted by suffix + hereafter) and clockwise (-) components of tidal velocities within the bottom boundary layer at a height z, $\mathbf{U}^{\pm}(z) = U^{\pm}(z) + i\,V^{\pm}(z)$, could be related with those outside the boundary layer, $\mathbf{U}_\infty^{\pm}$, using Kelvin functions ker and kei:

$$\mathbf{U}^{\pm}(z) = \mathbf{U}_\infty^{\pm}\left[\left(1 - \frac{\ker\xi^{\pm}(z)\ker\xi_0^{\pm} + \mathrm{kei}\xi^{\pm}(z)\mathrm{kei}\xi_0^{\pm}}{\ker^2\xi_0^{\pm} + \mathrm{kei}^2\xi_0^{\pm}}\right) \pm i\left(\frac{\ker\xi^{\pm}(z)\ \mathrm{kei}\xi_0^{\pm} - \mathrm{kei}\xi^{\pm}(z)\ker\xi_0^{\pm}}{\ker^2\xi_0^{\pm} + \mathrm{kei}^2\xi_0^{\pm}}\right)\right] \quad (3)$$

where $\xi^{\pm}(z) = 2|(f \pm \sigma)z/\kappa\hat{u}_*|^{1/2}$, $\xi_0^{\pm} = 2|(f \pm \sigma)z_0/\kappa\hat{u}_*|^{1/2}$and i is the imaginary unit.. Note that the factor 2 is missing in the definition of $\xi^{\pm}(z)$ and $\xi_0^{\pm}$ in equation (15) of Soulsby (1983)[7].

If we apply equation (3) at $z = 1$m and $z = z_M$, and eliminate $\mathbf{U}_\infty^{\pm}$, we will obtain a relation between the near-bottom tidal velocity $\mathbf{U}_b^{\pm} = \mathbf{U}^{\pm}(z = 1\mathrm{m})$ and the depth-averaged velocity $\mathbf{U}_M^{\pm} = \mathbf{U}^{\pm}(z = z_M)$:

$$\begin{pmatrix} U_b^{\pm} \\ V_b^{\pm} \end{pmatrix} = \begin{pmatrix} \Phi_A^{\pm} & \pm\Phi_B^{\pm} \\ \mp\Phi_B^{\pm} & \Phi_A^{\pm} \end{pmatrix} \begin{pmatrix} U_M^{\pm} \\ V_M^{\pm} \end{pmatrix} \quad (4)$$

where

$$\Phi_A^{\pm} = \frac{1}{AB_M}\left((\ker\xi_0^{\pm} - \ker\xi_M^{\pm})(\ker\xi_0^{\pm} - \ker\xi_b^{\pm}) + (\mathrm{kei}\,\xi_0^{\pm} - \mathrm{kei}\,\xi_b^{\pm})(\mathrm{kei}\,\xi_0^{\pm} - \mathrm{kei}\,\xi_b^{\pm})\right) \quad (5)$$

$$\Phi_B^{\pm} = \frac{1}{AB_M}\left(\ker\xi_0^{\pm}(\mathrm{kei}\,\xi_b^{\pm} - \mathrm{kei}\,\xi_M^{\pm}) + \mathrm{kei}\,\xi_0^{\pm}(\ker\xi_M^{\pm} - \ker\xi_b^{\pm}) + (\ker\xi_b^{\pm}\ \mathrm{kei}\,\xi_M^{\pm} - \ker\xi_M^{\pm}\ \mathrm{kei}\,\xi_b^{\pm})\right) \quad (6)$$

$$AB_M = (\ker\xi_0^{\pm} - \ker\xi_M^{\pm})^2 + (\mathrm{kei}\,\xi_0^{\pm} - \mathrm{kei}\,\xi_M^{\pm})^2 \quad (7)$$

Finally, the near-bottom tidal velocities (u_b, v_b), defined at the level 1m above the bottom, are derived by adding the anti-clockwise and clockwise components of the tidal velocity.

$$u_b = U^+ + U^-,\ v_b = V^+ + V^- \quad (8)$$

2.3 Wave model

The near-bottom orbital velocity of wind waves used in the bottom-stress calculation was obtained from the output of a third-generation wave model[8] (WAVE WATCH-III, version 3.14). Firstly, the model was applied to a global domain covering the latitudes from 77°S to 80°N with a spatial resolution of 1.25 degrees (zonal) and 1.00 degrees (meridional). The output of the global model was then used as a boundary value of a regional simulation having a spatial resolution of 1/12 degree in both zonal and meridional directions. As for the wind forcing, we used NOAA/GFS4 reanalysis dataset which was supplied for every hour with a spatial resolution of 0.3125 degree. The high temporal resolution is necessary to resolve resuspension events, and the high spatial resolution is essential to reconstruct waves in enclosed embayment such as Bohai Bay and upper Gulf of Thailand.

Instead of estimating the bottom orbital velocity of a single representative wave by using significant wave heights and periods, we adopted a root-mean square value of the bottom orbital velocity averaged over a wave spectrum, u_{bw}, which is available as an output of the wave model.

$$u_{bw} = \left[2 \iint \frac{\sigma^2}{\sinh^2 kd} F(k,\theta)\, dk d\theta \right]^{\frac{1}{2}} \qquad (9)$$

where σ is the (intrinsic) wave frequency, k the wave number, d the water depth, θ the wave direction and $F(k,\theta)$ the wave spectrum.

2.4 Bottom-stress estimation

Maximum bottom stresses over a wave period under the presence of waves and tidal currents were calculated by using equation (69) of Soulsby (1997)[9], which is:

$$\tau_{\max} = [(\tau_m + \tau_w \cos\phi)^2 + (\tau_w \sin\phi)^2]^{1/2} \qquad (10)$$

where

$$\tau_m = \tau_c \left[1 + 1.2 \left(\frac{\tau_w}{\tau_c + \tau_w} \right)^{3.2} \right] \qquad (11)$$

and $\tau_w = (1/2)\rho f_w (u_{bw})^2$ is wave-only peak bottom stress, ρ (=1027kg/m^3) the density of seawater, $\tau_c = \rho c_D \left(u_b^2 + v_b^2\right)^{1/2}$ a bottom stress induced solely by a tidal current, ϕ the direction of a significant wave relative to a tidal current, respectively. The wave friction factor f_w was calculated by employing a numerical code of Signell et al. (1990)[10].

$$f_w = \max\{ f_{wr}, f_{ws} \} \qquad (12)$$

where the rough bed friction factor

$$f_{wr} = 0.237 \cdot (k_{br}/A)^{0.52} \qquad (13)$$

the smooth bed friction factor

$$f_{ws} = \begin{cases} 0.0521\, R_w^{-0.187} & (R_w > 5\times10^5) \\ 2\, R_w^{-0.5} & (1\times10^{-5} < R_w \le 5\times10^5) \\ 0 & (R_w < 1\times10^{-5}) \end{cases} \qquad (14)$$

and k_{br} $(= 30\, z_0)$ the Nikuradse equivalent grain roughness, $A = u_{bw}T_p/2\pi$ the semi-orbital excursion, T_p the peak wave periods, $R_w = u_{bw}A/\nu$ the wave Reynolds number and $\nu(= 1.36\times10^{-6}\ \mathrm{m/s^2})$ the kinematic viscosity, respectively.

3. Results

As an example, we present a case when the procedure was applied to the Yellow/East China Sea to verify its performance. The bottom stress due to waves and tides were estimated at every hour from November 1992 to December 2009 with a spatial resolution of 1/12 degrees.

3.1 Tidal model

The tidal model used in the Yellow/East China Sea case covers a rectangular area covering longitudes from 117°E to 131°05'E and latitudes from 23°55'N to 42°N. The root mean square difference between predicted and observed values at 228 tide-gauge stations listed in Admiralty Tide Table (2000 edition) were 0.13m (0.05m) for amplitudes and 22.8 degree (17.6 degree) for phases of M_2 (K_1) constituents, respectively.

It is to be noted that some part of the root-mean-square (rms) differences could be ascribed to the uncertainty in observed values, as they are measured at different periods and durations, and may have influenced by local conditions around the tide-gauge stations. For example, M_2 amplitude and phase at Kunsan outer port (station no. 7504) and Kunsan (7505) stations differ by 0.18m and 14degree, respectively, even though two stations are only 7km apart and fall in a same model grid cell. As Kunsan Port has experienced a large expansion in the last century, difference in the period used for tidal analysis at two stations may have contributed to such a large discrepancy in tidal harmonic constants.

Figure 1 compares predicted oceanic currents and observed[11] tidal currents at a mid-shelf region in the East China Sea, which were in good agreement with each other. While the current velocity is dominated by tidal components, offsets of meridional currents as large as 0.1m/s were observed on 7 May (Fig. 1). As a general circulation model predicts a burst of non-tidal flow toward NNE direction as large as 0.1m/s on that day[12], the offset is probably due to such a subtidal currents. The amplitude of M_2 tidal velocity at this site is 0.4m/s, which is about 2/3 of the maximum speed observed. It is therefore suggested that components other than M_2 would be necessary to estimate the effect of tides.

Near-bottom tidal currents derived by the method introduced in section 2.2 were compared with those observed at two sites around the Changjiang Estuary[13)] (Fig. 2). It is found that the observed and predicted values are consistent with each other.

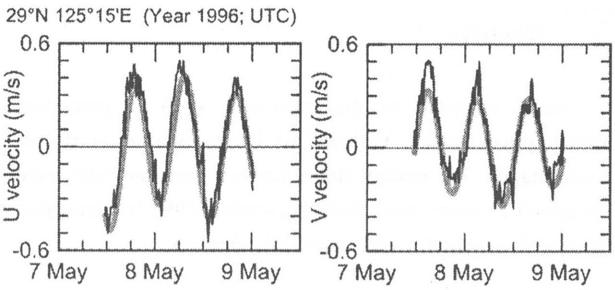

Fig. 1. Zonal (left) and meridional (right) current velocity at a location in the mid-shelf East China Sea (water depth 110m). Thin lines denote observed velocity measured by an ADCP averaged over lower 35m[11)] whereas thick gray lines indicate current velocity predicted by the tidal model.

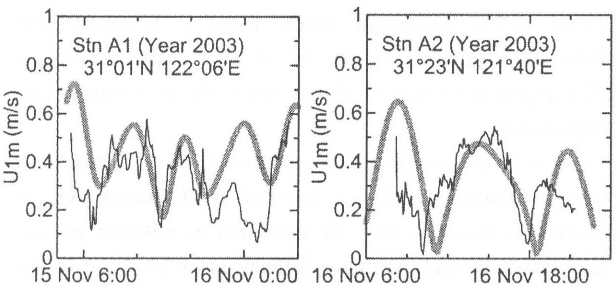

Fig. 2. Current speed at a layer 1m above the seafloor at two sites near the Changjiang Estuary, obtained by ADCP observations (thin lines) and by the tidal model (thick lines).

3.2 Wave model

In the Yellow/East China Sea case, the regional wave simulation was conducted at areas slightly smaller than those for the tidal model: longitudes from 117°30'E to 127°25'E and latitudes from 25°35'N to 41°N, while the spatial resolution remains the same (1/12degree). Fig. 3 compares the maximum wave height observed by a buoy in the northern Yellow Sea[14)] with those predicted by the wave model. It is shown that the model were able to produce a rapid increase of the maximum wave height taken place within a day, induced by the passage of a depression, and a peak value ranging about 11m.

3.3 Bottom-stress estimation

Comparison between suspended sediment concentrations (SSCs) observed in the southwestern Yellow Sea and bottom stress predicted under the presence of waves and tides is shown in Fig. 4. It is found that the temporal pattern of the predicted bottom stress is consistent with that of the SSCs observed. The model results indicates that the highest peak of SSC observed at around 10:00 was due to the combined effect of strong tidal currents and increased wave heights , suggesting the significance of considering both tidal and wave impacts when estimating the occurrence of resuspension. Discrepancies among the timing of smaller peaks found at 02:00 and 13:00 were caused because the timing of the predicted flood tides lagged behind those actually observed (not shown but consistent with the pattern of SSCs), even though the timing of ebb tides were consistent among predicted and observed. This discrepancy may be due to the localiized tidal modification at this site, which is situated on the flank of a large tidal sand ridge.

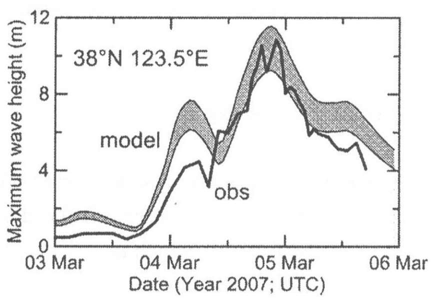

Fig. 3. Maximum wave height observed at the northern Yellow Sea (solid line, State Oceanic Administration Buoy No.15[14)]) and those predicted by the wave model (hatched). The predicted maximum wave height was derived by multiplying the predicted significant wave height by a factor of 1.6-2.0.

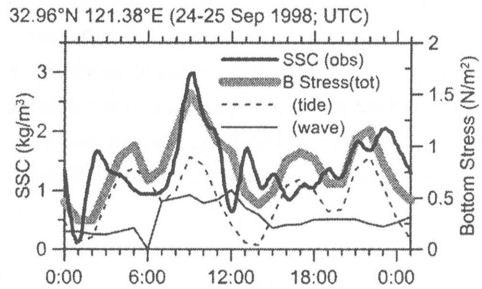

Fig. 4. Suspended sediment concentration (SSC) in a near-bottom layer observed at Station 14 in the southwestern Yellow Sea[15)] (thick solid line) and bottom stresses predicted by the method proposed in this report, which considers the presence of waves and tides (thick gray), tides only (dotted), and waves only (thin solid).

5. Summary and discussion

In this report, a method to estimate the bottom stress induced by waves and tides, aimed to estimate the occurrence of sediment resuspension over the whole area of the continental shelf take place in a temporal range of years, was developed. Comparison between model outputs and observed results at the Yellow/East China Sea indicated that (1) a large portion of changes in near-bottom SSCs on the continental shelf could be reproduced from the temporal pattern of bottom stresses due to the combined effect of wave and tides, (2) the model needs to resolve extreme events which have a time scale of several hours, and (3) the tidal model should imply tidal constituents other than M2. Though the bottom stress is one of the main factors which induce sediment resuspensions, there are several other points, such as the grain size, cohesiveness, and water content of sediments, bedform features, water temperatures, etc., which affects the occurrence of resuspension, the current model may be applied to estimate the overall statistics over the continental shelf.

Acknowledgement

This study was supported by the Japan Society for the Promotion of Science (KAKENHI 23510009).

References

1) T. Yanagi, S. Takahashi, A. Hoshika and T. Tanimoto, J. Oceanogr. 52(1996)539.
2) T. Wei, Z. Chen, L. Duan, J. Gu, Y. Saito, W. Zhang, Y. Wang and Y. Kanai, Estuar. Coast. Shelf Sci. 71(2007)37.
3) T. Yanagi and K. Inoue, J. Oceanogr. 51(1995)537.
4) M. Watanabe, Estuar. Coast Shelf Sci. 71(2007)81.
5) Y. Zhu and R. Chang, Estuar. Coast. Shelf Sci. 51(2000)663.
6) P. Bills and J. Noye, In: Numerical Modelling: Applications to Marine Systems, J. Noye ed., North-Holland Mathematics Studies 145, Elsevier, (1987).
7) R.L. Soulsby, In: Physical Oceanography of Coastal and Shelf Seas, ed. B. Johns, Elsevier (1983)189.
8) T.L. Tolman, NOAA/NWS/NCEP/MMAB technical note 222 (2002).
9) R.L. Soulsby, Dynamics of Marine Sands, Thomas Telford (1997).
10) R.P. Signell, R.C. Beardsley, H.C. Graber and A. Capotondi, J. Geophys. Res. 95(1990)9671.
11) Z.X. Liu, S. Berné, Y. Saito, H. Yu, A. Trentesaux, K. Uehara, P. Yin, J.P. Liu, C. Li, G. Hu and X. Wang, Cont. Shelf Res. 27(2007)1820.
12) Y. Miyazawa, R. Zhang, X. Guo, H. Tamura, D. Ambe, J.-S. Lee, A. Okuno, H. Yasunari, T. Setou and K. Komatsu, J. Oceanogr. 65(2009)737.
13) J. Gao, Y. Yang, Y. Wang, S. Pan, R. Zhang, Front. Earth Sci. China 2(2008)249.
14) State Oceanic Administration, China, 2007 China Marine Disaster Bulletin (issued at January 2008), http://www.soa.gov.cn/soa/hygb/zhgb/webinfo/2008/01/1271382648975667.htm.
15) D. Wu and R. Zhang, J. Sed. Res., 9(2007)42.